DOI: 10.4081/aiua.2026.15133

ORIGINAL PAPER

Diagnostic performance of PI-RADS and PSA density for detecting clinically significant prostate cancer

Walid Shanaa [1], Ibrahim Alnadhari [1, 2], Omar Ali [1, 2], Osama Abdeljaleel [1, 2], Hana J. Abukhadijah [3], Ahmad Shamsodini [1, 2]

[1] Urology Section, Department of Surgery, Al Wakra Hospital, Hamad Medical Corporation, Qatar;
[2] Department of Surgery, Qatar University, Qatar;
[3] Academic Health System Department, Hamad Medical Corporation, Qatar.

Summary *Background: Multiparametric magnetic resonance imaging (mpMRI), interpreted using the Prostate Imaging Reporting and Data System (PI-RADS), is increasingly used to improve prostate cancer detection and reduce unnecessary biopsies. However, its diagnostic accuracy compared with histopathological confirmation remains variable across institutions. This study aimed to evaluate the correlation between mpMRI findings and TRUS-guided prostate biopsy results in detecting clinically significant prostate cancer (csPCa) in our patient cohort.*

Methods: This retrospective diagnostic accuracy study included 100 biopsy records (86 unique patients) who underwent mpMRI followed by TRUS-guided biopsy. mpMRI findings were scored using PI-RADS v2, while biopsy histopathology served as the reference standard. Clinically significant prostate cancer (csPCa) was defined as ISUP Grade Group ≥ 2. Diagnostic performance was assessed for two interpretive rules: (1) Baseline rule: PI-RADS ≥ 4 as positive; (2) Combined rule: PI-RADS ≥ 4 or PI-RADS = 3 with PSA density (PSAD) > 0.15 ng/mL/mL. Sensitivity, specificity, predictive values, and area under the ROC curve (AUC) were calculated. Hierarchical logistic regression assessed the independent contribution of PSAD and clinical covariates.

Results: Malignant cases showed higher PSA (median 10.0 ng/mL vs 7.0 ng/mL) and PSAD (0.32 vs 0.13 ng/mL/mL) and smaller prostate volumes (36.5 mL vs 61.0 mL) compared with benign cases. csPCa detection increased with rising PI-RADS category (3.7% for PI-RADS 3, 56.9 % for PI-RADS 4-5). At the patient level, the Baseline rule achieved sensitivity = 86.7% and specificity = 66.1%, while the Combined rule increased sensitivity to 90.0 % with specificity = 55.4%. The ordinal PI-RADS score demonstrated excellent discrimination (AUC = 0.826, 95% CI 0.713-0.924). In logistic regression, adding PSAD improved model AUC from 0.836 to 0.888 ($p < 0.001$), and inclusion of age and prostate volume further increased AUC to 0.900 ($p = 0.044$). Within PI-RADS 3 lesions, the optimal PSAD threshold (Youden index) was 0.163 ng/mL/mL, yielding 100% sensitivity and 76% specificity. Post-biopsy complications were within expected ranges, with mild hematuria (29%), minor rectal bleeding (23%), and UTI (7%) being most common.

Conclusions: mpMRI findings strongly correlated with histopathological outcomes from TRUS-guided biopsy. Incorporating PSA density significantly enhanced the diagnostic accuracy for csPCa, particularly in equivocal PI-RADS 3 cases. Combining mpMRI and PSAD can refine patient selection for biopsy and improve early detection of clinically significant prostate cancer.

KEY WORDS: Prostate cancer; mpMRI; PI-RADS; TRUS-guided biopsy; PSA density; Diagnostic accuracy.

Submitted 8 March 2026; Accepted 26 March 2026

INTRODUCTION

Prostate cancer (PCa) remains one of the most frequently diagnosed malignancies among men and continues to impose a major global health burden, highlighting the need for accurate diagnostic pathways (1). Although PSA screening has improved early detection, its limited specificity results in unnecessary biopsies and overdiagnosis of indolent disease (2). The widely used *transrectal ultrasound-guided biopsy* (TRUS-Bx) also has notable limitations, including random sampling, suboptimal visualization of anterior and apical tumors, and underdetection of *clinically significant prostate cancer* (csPCa) (3-5), contributing to misclassification and persistent diagnostic uncertainty (6, 7).

Multiparametric MRI (mpMRI) has transformed prostate cancer evaluation, with the PI-RADS standard providing a validated likelihood score for clinically significant disease (8, 9). Robust multicenter studies have shown strong associations between PI-RADS categories and adverse pathological features after radical prostatectomy (10-14). Major trials have established mpMRI as a pivotal triage tool, reducing unnecessary biopsies while improving detection of significant cancers (15-17). However, diagnostic performance varies, particularly for indeterminate PI-RADS 3 lesions. To address this, *PSA density* (PSAD) has emerged as a critical adjunct, refining risk stratification by correcting for gland volume (20, 21).

Nevertheless, the performance of mpMRI is not uniform across institutions, being influenced by variations in scanner technology, acquisition protocols, and radiologist expertise (18, 19). This variability creates diagnostic uncertainty, which is most pronounced for PI-RADS category 3 lesions. To address this limitation, *prostate-specific*

antigen density (PSAD) has gained prominence as a valuable adjunct, improving specificity by accounting for gland volume, particularly in equivocal cases (20, 21). Beyond imaging, clinical parameters like age and PSA remain central to risk stratification, as reflected in contemporary EAU and NCCN guidelines that advocate for an integrated, multi-parameter diagnostic approach (22-25). This is especially relevant given that TRUS-guided biopsy carries non-trivial risks, including infectious complications exacerbated by rising antimicrobial resistance (26). Accordingly, this study evaluates the diagnostic performance of mpMRI using PI-RADS v2.0 in correlation with TRUS-guided biopsy histopathology. We further assess the additive value of PSA density and prostate volume to determine whether an integrated multi-parameter approach can improve discrimination of clinically significant disease and refine biopsy decision-making in contemporary prostate cancer diagnostics.

Methods

Study design and reporting

This was a retrospective diagnostic accuracy study designed to assess the ability of *multiparametric magnetic resonance imaging* (mpMRI), interpreted using the *Prostate Imaging Reporting and Data System* (PI-RADS), to detect *clinically significant prostate cancer* (csPCa). The histopathological findings from *transrectal ultrasound* (TRUS)-guided prostate biopsy served as the reference standard. All stages of study design, data processing, and analysis adhered to recognized methodological standards and were reported in accordance with the STAndards for Reporting of Diagnostic Accuracy Studies (STARD 2015) and the STROBE statement for observational research. These frameworks guided the transparent description of participants, index test, reference standard, and statistical methodology.

Data source and patient selection

Data were retrieved from a prospectively maintained institutional TRUS-biopsy dataset at urology department at Al Wakra hospital from 01/07/2017 to 30/03/2024 and harmonized into a workbook containing record-level and patient-level sheets. Each record represented one biopsy event with corresponding mpMRI findings. To avoid duplication, a patient-level dataset was derived by retaining a single representative record per individual. The selection hierarchy favored cases with positive biopsy results, higher *International Society of Urological Pathology* (ISUP) grade group, higher PI-RADS score, and complete PSAD information. Patients lacking mpMRI data or biopsy results were excluded.

Index test and reference standard

The index test was mpMRI interpreted by experienced radiologists following PI-RADS version 2 criteria, with scores ranging from 1 (very low likelihood of clinically significant cancer) to 5 (very high likelihood). The reference standard was the histopathological result of TRUS-guided prostate biopsy. The primary outcome, csPCa, was defined as ISUP grade group ≥ 2 (Gleason score ≥ 3+4). Cases with ISUP 1 or negative biopsies were considered negative for csPCa. Biopsy-positive cases without an available grade (none in this dataset) were prespecified for exclusion from csPCa-specific analyses but retained in sensitivity analyses evaluating any prostate cancer detection.

Derived variables and diagnostic rules

Prostate volume was extracted from imaging reports and recorded in milliliters. PSA density was calculated as total serum PSA divided by prostate volume (ng/mL/mL). Two diagnostic rules were evaluated. The Baseline rule defined a positive mpMRI as PI-RADS ≥ 4. The Combined rule incorporated PSA density by defining a positive mpMRI as PI-RADS ≥ 4 or PI-RADS = 3 with PSAD > 0.15. These thresholds were selected from prior evidence and validated through empirical evaluation within the dataset.

Statistical analysis

Diagnostic accuracy for both rules was quantified using sensitivity, specificity, positive and negative predictive values, and positive and negative likelihood ratios, each reported with 95% *confidence intervals* (CIs) derived from Wilson score methods. ROC curve analysis was performed using the ordinal PI-RADS score (1-5) as a continuous predictor to determine the *area under the curve* (AUC) and corresponding 95% bootstrap CIs. Differences in paired misclassification between the Baseline and Combined rules were assessed using McNemar's exact test.

To explore PSA density as an independent biomarker, group comparisons were conducted using the Mann-Whitney U test for csPCa *versus* non-csPCa and the Kruskal-Wallis test across PI-RADS categories. Within the PI-RADS 3 subgroup, an optimal PSAD cutpoint was determined by maximizing the Youden index, with comparisons against pre-specified thresholds (0.10, 0.15, and 0.20).

Multivariable logistic regression was used to quantify independent associations with csPCa. Three hierarchical models were fitted sequentially: Model 1 included PI-RADS alone, Model 2 added PSAD, and Model 3 further incorporated age and prostate volume. All models were restricted to complete cases with non-missing data on these variables, ensuring consistent sample size and event count across comparisons. Improvements in model performance were assessed using *likelihood ratio* (LR) tests between sequentially nested models, and model discrimination was summarized using AUCs with 95% bootstrap CIs. The analysis was performed using RStudio statistical software with R version 4.4.2, and Python 3.11.

Results

Baseline characteristics

At the record level (n = 100), malignant or any cancer records demonstrated higher PSA and PSAD values and smaller prostate volumes than benign or negative biopsy records. Median PSA was 10.0 ng/mL (IQR 7.22-17.00) in malignant cases compared with 7.0 ng/mL (6.00-10.30) in benign cases, while median prostate volume was 36.5 mL versus 61.0 mL. The resulting PSA density was 0.32 ng/mL/mL for malignant cases and 0.13 ng/mL/mL for benign cases. Higher PI-RADS categories

Table 1.
Baseline characteristics of study records by biopsy outcome.

Variable	Benign/ No cancer (n = 62)	Malignant/ Any cancer (n = 38)
Demographics:		
Age, years	60.00 (56.00-67.00)	63.50 (55.50-69.00)
Clinical Characteristics:		
PSA, ng/mL	7.00 (6.00-10.30)	10.00 (7.22-17.00)
Prostate volume, mL	61.00 (42.00-97.00)	36.50 (27.25-55.00)
PSAD, ng/mL/mL	0.13 (0.09-0.15)	0.32 (0.17-0.61)
Digital Rectal Examination:		
Benign feeling	55 (88.7%)	15 (39.5%)
Asymmetrical	4 (6.5%)	7 (18.4%)
Right nodule	2 (3.2%)	6 (15.8%)
Hard nodule	0 (0.0%)	2 (5.3%)
Left lobe nodule	0 (0.0%)	2 (5.3%)
Left lobe hard nodule	0 (0.0%)	1 (2.6%)
Left side nodule	1 (1.6%)	0 (0.0%)
Not done	0 (0.0%)	1 (2.6%)
Missing	0 (0.0%)	4 (10.5%)
Family History of Prostate Cancer:		
No	52 (83.9%)	33 (86.8%)
Yes, father	6 (9.7%)	4 (10.5%)
Yes, brother	2 (3.2%)	1 (2.6%)
Yes (unspecified)	1 (1.6%)	0 (0.0%)
Missing	1 (1.6%)	0 (0.0%)
MRI Characteristics:		
PI-RADS score:		
1	1 (1.6%)	1 (2.6%)
2	15 (24.2%)	3 (7.9%)
3	23 (37.1%)	4 (10.5%)
4	19 (30.6%)	10 (26.3%)
5	2 (3.2%)	20 (52.6%)
Missing	0 (0.0%)	0 (0.0%)
Lesion size, mm	9.50 (8.00-13.00)	18.00 (11.50-22.00)
Periprostatic invasion:		
Absent	61 (98.4%)	25 (65.8%)
Present	0 (0.0%)	13 (34.2%)
Missing	0 (0.0%)	0 (0.0%)

Data presented as median (interquartile range) for continuous variables and n (%) for categorical variables. Record-level analysis (n = 100); patient-level diagnostic accuracy analysis (n = 88) presented in subsequent tables.
DRE: digital rectal examination; IQR: interquartile range; MRI: magnetic resonance imaging; PI-RADS: Prostate Imaging Reporting and Data System; PSA: prostate-specific antigen; PSAD: prostate-specific antigen density.

Figure 1.
Forest plot comparing diagnostic accuracy of baseline and combined classification rules.

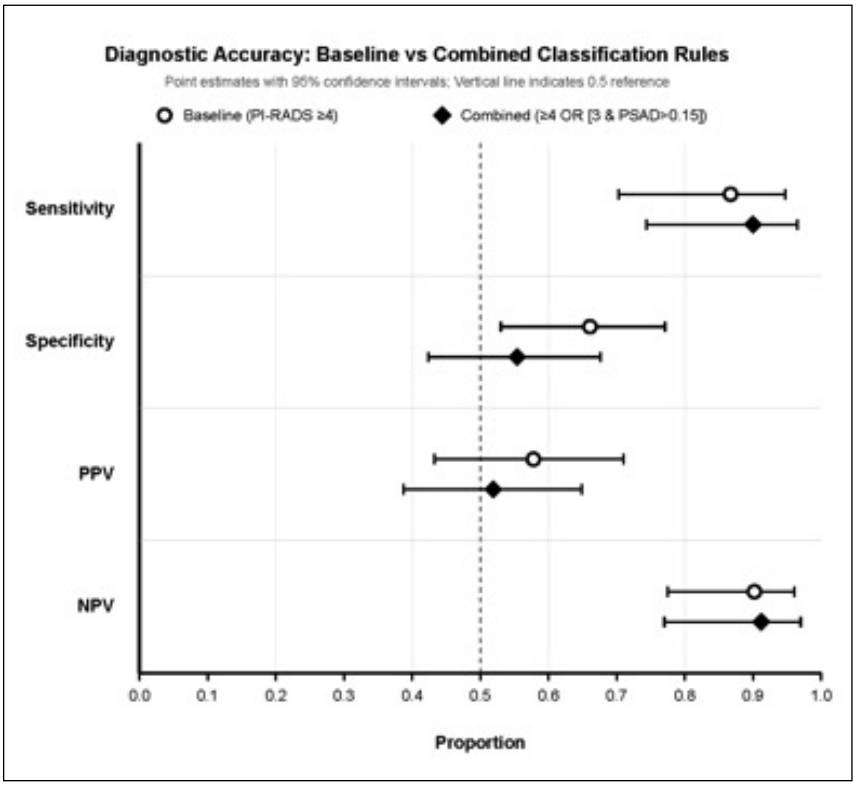

were strongly associated with malignant outcomes: PI-RADS 5 comprised 52.6 % of malignant/any cancer records but only 3.2 % of benign records. Digital rectal examination abnormalities and periprostatic invasion were also more frequent among malignant records, as detailed in Table 1 and Figure 1.

Diagnostic performance and discrimination

Record-level PI-RADS risk stratification revealed a progressive increase in csPCa detection with rising PI-RADS category, from 3.7 % in equivocal (PI-RADS 3) to 56.9 % in high-risk (PI-RADS 4-5) lesions, whereas low-risk PI-RADS 1-2 showed only 15 % detection. At the patient level (n = 86 with non-missing PI-RADS), the Baseline rule (PI-RADS ≥ 4) achieved sensitivity = 0.867 (95 % CI 0.703-0.947) and specificity = 0.661 (0.530-0.771). The Combined rule increased sensitivity to 0.900 (0.744-0.965) but reduced specificity to 0.554 (0.424-0.676). McNemar's test indicated no significant difference in misclassification between the two rules.

The full ordinal PI-RADS scale yielded an AUC = 0.826 (95 % CI 0.713-0.924). In hierarchical logistic regression based on the 85-patient complete-case subset (30 events = csPCa positive), Model 1 (PI-RADS only) achieved AUC = 0.836 (95 % CI 0.724-0.930). Adding PSAD (Model 2) improved AUC to 0.888 (95 % CI 0.818-0.966; LR test P-value < 0.001), while adding age and prostate volume (Model 3) further increased AUC to 0.900 (95 % CI 0.846-0.977; LR test P-value = 0.044). These findings are summarized in Table 2, and Figure 2 illustrates ROC curves for the three hierarchical models.

PSA density analyses and optimal thresholding

PSAD was significantly higher in patients with csPCa (median = 0.321 ng/mL/mL) than in those without (median = 0.128 ng/mL/mL; Mann-Whitney U = 1463.0, P-value < 0.001). Across PI-RADS categories, PSAD values increased stepwise from a median = 0.129 in PI-RADS 2 to 0.593 in PI-RADS 5 (Kruskal-Wallis H = 27.42, P-value < 0.001). In the PI-RADS 3 subgroup (n = 22), the optimal PSAD cutpoint determined by the

Table 2.
Diagnostic performance, model comparison, and PI-RADS risk stratification.

Analysis Component	Category/Model	Number of Individuals	Value 1	Value 2	Value 3	Value 4	Value 5	Value 6
PI-RADS Risk Stratification (Record-Level)			**csPCa−**	**csPCa+**	**Total**	**Detection Rate (%)**	**–**	**–**
	Low Risk (PI-RADS 1–2)	20	17	3	20	15.0	–	
	Equivocal (PI-RADS 3)	27	26	1	27	3.7	–	
	High Risk (PI-RADS 4–5)	51	22	29	51	56.9	–	
Classification rule diagnostic accuracy (Patient-Level)			**Sensitivity (95% CI)**	**Specificity (95% CI)**	**PPV (95% CI)**	**NPV (95% CI)**	**LR+**	**LR-**
	Baseline (PI-RADS ≥ 4)	86	0.867 (0.703–0.947)	0.661 (0.530–0.771)	0.578 (0.433–0.710)	0.902 (0.775–0.961)	2.554	0.202
	Combined (≥ 4 OR [3 & PSAD > 0.15])	86	0.900 (0.744–0.965)	0.554 (0.424–0.676)	0.519 (0.387–0.649)	0.912 (0.770–0.970)	2.016	0.181
Discriminative Performance (Patient-Level)			**Events**	**AUC**	**95% CI**	**Comparison**	**LR p-value**	**–**
	PI-RADS score (1–5)	86	30	0.826	0.713–0.924	–	–	–
	Model 1: PI-RADS only	85	30	0.836	0.724–0.930	Reference	–	–
	Model 2: PI-RADS + PSAD	85	30	0.888	0.818–0.966	vs Model 1	< 0.001	–
	Model 3: PI-RADS + PSAD + Age + Volume	85	30	0.900	0.846–0.977	vs Model 2	0.044	–

Risk stratification demonstrates PI-RADS 4–5 lesions had 15-fold higher csPCa detection versus PI-RADS 3 (56.9% vs 3.7%). Combined rule achieved higher sensitivity (90.0% vs 86.7%) but lower specificity (55.4% vs 66.1%) compared to Baseline; McNemar test p = 0.125. Adding PSAD to PI-RADS significantly improved discrimination (Model 2 vs 1: p<0.001); clinical variables provided additional improvement (Model 3 vs 2: p = 0.044).
AUC: area under the receiver operating characteristic curve; CI: confidence interval; csPCa: clinically significant prostate cancer; LR: likelihood ratio; LR+: likelihood ratio positive; LR−: likelihood ratio negative; NPV: negative predictive value; PI-RADS: Prostate Imaging Reporting and Data System; PPV: positive predictive value; PSAD: prostate-specific antigen density.

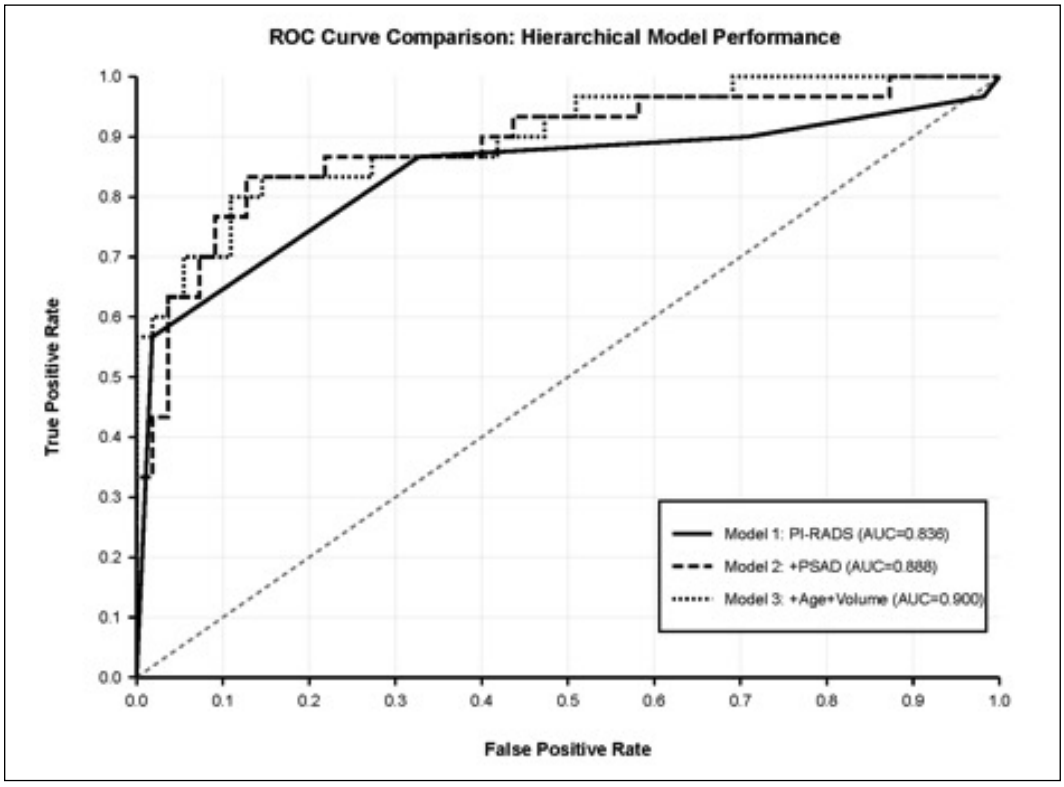

Figure 2.
ROC curves illustrating discrimination of Models 1, Model 2 and Model 3.

Youden index was 0.163, corresponding to sensitivity = 1.000 and specificity = 0.762. The pre-specified thresholds 0.10, 0.15, and 0.20 demonstrated the expected sensitivity-specificity trade-off patterns shown in Table 3.

The distribution of PSAD by PI-RADS category, represented as medians with interquartile range whiskers and a dashed clinical threshold line at 0.15 ng/mL/mL, is illustrated in Figure 3.

Table 3.
PSA density as independent biomarker for clinically significant prostate cancer.

Analysis	Category/Group	Median PSAD (ng/mL/mL)	Q1	Q3	Number of individuals	Test statistic	P-value
PSAD by csPCa Status	csPCa-positive	0.321	–	–	30	U = 1463.000 (Mann-Whitney)	< 0.001
	csPCa-negative	0.128	–	–	57		
PSAD by PI-RADS Category	PI-RADS 1	0.364	0.363	0.365	2	H = 27.420 (Kruskal-Wallis)	< 0.001
	PI-RADS 2	0.129	0.112	0.169	17		
	PI-RADS 3	0.124	0.093	0.168	22		
	PI-RADS 4	0.140	0.110	0.228	26		
	PI-RADS 5	0.593	0.246	0.685	18		
Optimal PSAD Cutpoint for PI-RADS 3 Lesions	0.163 (Youden-optimal)	Sensitivity: 1.000	Specificity: 0.762	PPV: 0.167	n = 22	Youden Index: 0.762	–
	0.10 threshold	Sensitivity: 1.000	Specificity: 0.429	PPV: 0.077			
	0.15 threshold	Sensitivity: 1.000	Specificity: 0.714	PPV: 0.143			
	0.20 threshold	Sensitivity: 0.000	Specificity: 0.810	PPV: 0.000			

PSAD significantly higher in csPCa-positive patients and varies across PI-RADS categories. Optimal cutpoint analysis for PI-RADS 3 subgroup limited by small event count (n=1 csPCa case among 22 PI-RADS 3 patients). Patient-level analysis. csPCa: clinically significant prostate cancer; H: Kruskal-Wallis test statistic; PI-RADS: Prostate Imaging Reporting and Data System; PPV: positive predictive value; PSAD: prostate-specific antigen density; Q1: first quartile; Q3: third quartile; U: Mann-Whitney U statistic.

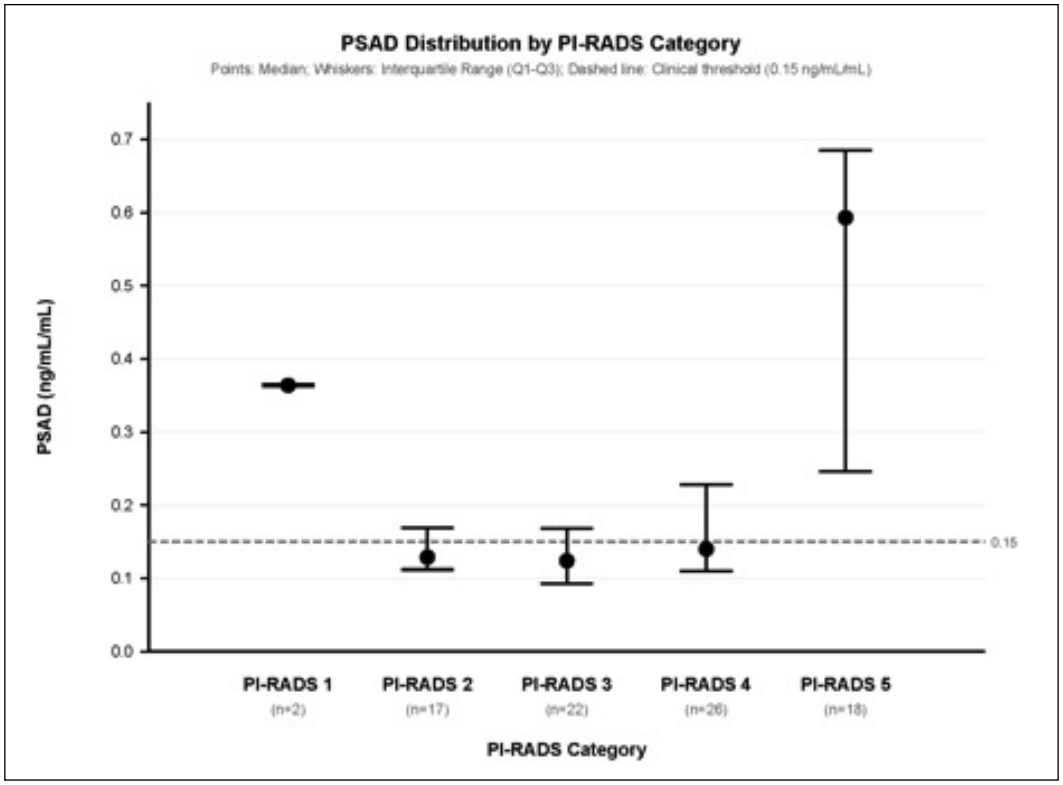

Figure 3.
Distribution of PSA density by PI-RADS category.

Table 4.
Post-biopsy complications following transrectal ultrasound-guided prostate biopsy.

Complication	Patients at Risk (n)	Events (n)	Proportion (%)	95% CI
Hematuria	99	29	29.3	21.2–38.9
Rectal bleeding	99	23	23.2	16.0–32.5
Urinary retention	98	21	21.4	14.5–30.5
Hematospermia	98	10	10.2	5.6–17.8
UTI	98	7	7.1	3.5–14.0
Sepsis	98	1	1	0.2–5.6

Proportions calculated with Wilson score 95% confidence intervals. Minor variations in sample size reflect case-specific missing data for each complication assessment. Record-level analysis. CI: confidence interval.

Post-biopsy complications

Post-biopsy complication rates were within expected ranges (Table 4).

The most frequent events were hematuria (29.3%) and rectal bleeding (23.2%); importantly, these were minor and self-limiting complications that resolved with con-

servative management. No patients required blood transfusion, hospital admission, or invasive intervention for bleeding-related events. Urinary retention (21.4%) was also managed conservatively. Only one case of sepsis was recorded in the cohort, corresponding to a low incidence rate. Minor variations in denominators reflected case-specific missingness for certain outcomes.

Discussion

In this retrospective cohort of 100 patients undergoing mpMRI followed by TRUS-guided biopsy for suspected prostate cancer, 40% were confirmed malignant, consistent with detection rates reported in similar clinical cohorts. A key finding of our study is the significant inverse association between prostate volume and malignancy risk, with malignant cases demonstrating markedly smaller prostates compared with benign cases. This observation supports prior evidence indicating that cancer is more readily detected in smaller glands where reduced benign prostatic hyperplasia results in less PSA dilution and consequently higher PSAD (27). These findings underscore the need to consider prostate volume in risk stratification, particularly when interpreting mpMRI and PI-RADS assessments.

PI-RADS scoring in our cohort demonstrated strong discriminatory value, with PI-RADS 5 accounting for over half of malignant lesions, aligning with previous research validating the predictive capability of higher PI-RADS categories for csPCa detection. Nonetheless, PI-RADS 3 remained a diagnostic gray zone, exhibiting a low csPCa detection rate (3.7%), similar to the wide-ranging malignancy rates (12-33%) reported in the literature. The moderate overall concordance between mpMRI and biopsy, as reflected by our diagnostic AUC, is consistent with known limitations of both modalities. mpMRI performance may vary due to inter-reader variability, segmentation challenges, and difficulty in detecting small or infiltrative lesions (33-36), whereas TRUS-guided biopsy remains susceptible to sampling error and anatomical limitations. These findings reinforce the indispensable role of histopathological confirmation, especially in equivocal lesions.

A central contribution of our study is the clear diagnostic benefit of integrating PSAD with mpMRI-based PI-RADS classification. The Baseline rule (PI-RADS ≥ 4) already demonstrated high sensitivity for csPCa; however, adding a PSAD threshold of > 0.15 for PI-RADS 3 lesions increased sensitivity from 0.867 to 0.900, improving detection without a disproportionate loss in specificity. Furthermore, in the PI-RADS 3 subgroup, a Youden-optimized PSAD cutoff of 0.163 ng/mL/mL provided perfect sensitivity and strong specificity, reinforcing PSAD's utility in distinguishing benign from malignant lesions within this ambiguous category. These results align with prior work advocating PSAD thresholds between 0.15 and 0.20 to refine risk stratification and avoid unnecessary biopsies in PI-RADS 3 lesions (37, 38).

Hierarchical multivariable modeling further demonstrated the additive diagnostic value of incorporating clinical parameters into imaging-based assessment. PI-RADS alone achieved an AUC of 0.836, improving to 0.888 with the inclusion of PSAD and further to 0.900 upon adding age and prostate volume. These incremental gains emphasize the synergistic value of combining mpMRI with quantitative biomarkers and patient-specific variables. Our findings also corroborate the elevated PSA values observed in malignant cases, consistent with established PSA thresholds recommending biopsy referral at values above 5.7 µg/L for younger men and above 6.1 µg/L for older individuals (39). Additionally, nearly half of malignant patients exhibited normal *digital rectal examination* (DRE) findings, reaffirming that DRE alone lacks sufficient sensitivity and cannot replace mpMRI in evaluating patients with elevated PSA – consistent with NCCN and EAU guidance (40, 41).

Post-biopsy complication rates were within internationally reported ranges. The most frequent events – hematuria and rectal bleeding – were minor and self-limiting, requiring no blood transfusion, hospital admission, or invasive intervention and remains within published global variability described in systematic reviews (42). Only a single case of sepsis was recorded in the cohort, emphasizing the overall safety profile of the procedure in our setting. Nevertheless, infectious risk remains an important consideration with transrectal biopsy. A large contemporary cohort reported sepsis rates below 1% under multi-day prophylaxis, whereas other modern prospective studies show rates around 2-3% (43, 44). More recent randomized studies also suggest that, when appropriate prophylaxis is used, transrectal and transperineal biopsy routes have comparable infection rates (45-47). These findings highlight the importance of tailoring prophylactic strategies to local antimicrobial environments to minimize infectious complications (48, 49).

Taken together, our findings reinforce the growing con-

Declarations

Ethical approval and consent for participate: *This study was approved by the medical research center at Hamad Medical Corporation (MRC-01-24-462). The study was conducted in accordance with the principles of the Declaration of Helsinki.*

Availability of data and material: *The datasets generated during and/or analyzed during the current study are available from the corresponding author on reasonable request.*

Competing interests: *The authors declare no conflicts of interest.*

Funding: *This study received no external funding.*

Authors' contributions: *All authors contributed significantly to the conception and design of the study. Data collection and curation were performed by Walid Shanaa, and Ibrahim Alnadhari. Data analysis and interpretation were conducted by Ibrahim Alnadhari and Hana J. Abukhadijah. The initial draft of the manuscript was prepared by Walid Shanaa, Ibrahim Alnadhari, and Omar Ali with critical revision and intellectual input from all co-authors. Osama Abdeljaleel and Ahmad Shamsodini provided senior clinical oversight and supervision. All authors reviewed, approved the final version of the manuscript, and agreed to be accountable for all aspects of the work.*

Acknowledgments: *None.*

sensus that PSAD should be routinely integrated into prostate cancer diagnostic pathways alongside mpMRI. The demonstrated inverse association between prostate size and malignancy, the enhanced performance of combined PI-RADS and PSAD approaches, and the robust improvement seen with multivariable modeling highlight the value of a multi-parameter diagnostic strategy. While TRUS-guided biopsy remains essential for definitive diagnosis, the variability in complication rates – especially infection – underscores the need for optimized prophylaxis, careful patient selection, and consideration of alternative biopsy pathways where appropriate.

Limitations of the study should be acknowledged. The retrospective design introduces potential selection and information bias. This was a single-center study with a modest sample size, which may limit generalizability. TRUS-guided biopsy, while widely used, is subject to sampling errors and may underestimate true disease burden. MRI-targeted biopsy and radical prostatectomy correlation were not available.

Future prospective studies incorporating MRI-targeted biopsies, artificial intelligence-assisted MRI assessment, and genomic biomarkers may further refine the detection of clinically significant prostate cancer while minimizing unnecessary procedures and associated morbidity.

Conclusions

This study confirms that integrating PSA density (PSAD) with PI-RADS significantly improves the detection of clinically significant prostate cancer, most critically in indeterminate PI-RADS 3 lesions. A multivariable model combining PSAD, PI-RADS, and prostate volume demonstrated superior predictive accuracy over mpMRI alone, thereby refining risk stratification to reduce unnecessary biopsies.

References

1. Siegel RL, Miller KD, Jemal A. Cancer statistics, 2018. CA Cancer J Clin. 2018; 68:7-30.

2. Zhu M, Liang Z, Feng T, et al. Up-to-date imaging and diagnostic techniques for prostate cancer: A literature review. Diagnostics. 2023; 13:2283.

3. Hodge KK, McNeal JE, Terris MK, Stamey TA. Random systematic versus directed ultrasound-guided transrectal core biopsies of the prostate. J Urol. 1989; 142:71-4.

4. Ortner G, Tzanaki E, Rai BP, et al. Transperineal prostate biopsy: the modern gold standard. Turk J Urol. 2021; 47(Suppl 1):S19-25.

5. Rebez G, Barbiero M, Simonato FA, et al. Targeted prostate biopsy: How, when, and why? Diagnostics. 2024; 14:1864.

6. Shaw GL, Thomas BC, Dawson SN, et al. Identification of pathologically insignificant prostate cancer is not accurate in unscreened men. Br J Cancer. 2014; 110:2405-11.

7. Abraham NE, Mendhiratta N, Taneja SS. Patterns of repeat prostate biopsy in contemporary practice. J Urol. 2015; 193:1178-84.

8. Turkbey B, Brown AM, Sankineni S, et al. Multiparametric prostate MRI in PCa. CA Cancer J Clin. 2016; 66:326-36.

9. Patel NU, Lind KE, Garg K, et al. Assessment of PI-RADS ≥3 for diagnosing csPCa. Abdom Radiol. 2019; 44:705-12.

10. Yamashiro JR, de Riese WT. Prostate volume vs cancer incidence: 30-year review. Res Rep Urol. 2021; 13:749-57.

11. Li W, Shang W, Lu F, et al. Diagnostic performance of EPE grading system. Front Oncol. 2022; 11:792120.

12. Jiang S, Li Y, Guo Y, et al. MRI-measured periprostatic fat ratio as risk factor. Sci Rep. 2024; 14:20896.

13. Liu WQ, Wei Y, Ke ZB, et al. MRI radiomics predicting pathological upgrading. Acad Radiol. 2024.

14. Kızılay F, Çelik S, Sözen S, et al. PI-RADS correlation with RP pathology: multicenter study. Prostate Int. 2020; 8:10-15.

15. Ahmed HU, El-Shater Bosaily A, Brown LC, et al. Diagnostic accuracy of mpMRI and targeted biopsy. Lancet. 2017; 389:815-22.

16. Kasivisvanathan V, et al. MRI-targeted biopsy vs standard TRUS biopsy. NEJM. 2018; 378:1767-77.

17. van der Leest M, et al. MRI-first pathway reduces biopsies. Lancet Oncol. 2019; 20:948-60.

18. Boesen L, et al. mpMRI diagnostic accuracy variability. Eur Urol Focus. 2022; 8:74-82.

19. Westphalen AC, et al. PI-RADS v2.1 performance. Radiology. 2021; 299:278-88.

20. Hansen NL, et al. PSAD thresholds improve PI-RADS 3 assessment. Eur Urol Oncol. 2021; 4:464-73.

21. Maggi M, et al. PSAD integration with mpMRI improves csPCa detection. Prostate Cancer Prostatic Dis. 2022; 25:1-9.

22. Loeb S, et al. PSA-based thresholds for biopsy. Eur Urol. 2014; 66:354-64.

23. Mottet N, et al. EAU Guidelines on Prostate Cancer. 2024 Edition.

24. NCCN Clinical Practice Guidelines in Oncology: Prostate Cancer. Version 2024.

25. Pilatz A, et al. Infection risk after TRUS biopsy. Eur Urol. 2020; 78:2-3.

26. Feliciano J, et al. Complications after transrectal biopsy. BJU Int. 2015; 116:173-9.

27. Briganti A, et al. Impact of prostate volume on the correlation between prostate-specific antigen level and prostate cancer detection. Eur Urol. 2007; 52:653-660.

28. Mehralivand S, et al. A grading system for extraprostatic extension on prostate MRI: detection and clinical outcomes. Radiology. 2019; 290:709-719.

29. Johnson LM, et al. Accuracy of multiparametric MRI for predicting extraprostatic extension in prostate cancer. AJR Am J Roentgenol. 2019; 213:W226-W235.

30. Taneja SS. Reconsidering nerve-sparing prostatectomy in MRI-defined extraprostatic extension. J Urol. 2018; 199:595-596.

31. Turkbey B, et al. Prostate Imaging Reporting and Data System version 2.1: 2019 update. Radiology. 2019; 292:400-403.

32. Park KJ, et al. PI-RADS category 3 lesions: cancer detection and management strategies. Urol Oncol. 2020; 38:573-582.

33. Sonn GA, et al. Targeted biopsy and misclassification in prostate cancer: limitations of MRI and TRUS biopsy. J Urol. 2013; 189:441-448.

34. Kasivisvanathan V, et al. MRI-targeted vs standard biopsy for prostate cancer detection: PRECISION trial. N Engl J Med. 2018; 378:1767-1777.

35. Moldovan PC, et al. Accuracy of MRI and PI-RADS for prostate cancer detection: systematic review. Eur Urol. 2017; 72:896-913.

36. Schoots IG, et al. MRI in early prostate cancer detection: meta-analysis. Eur Urol. 2015; 67:627-636.

37. Lo Gullo R, et al. Role of PSA density in PI-RADS 3 lesions. Radiology. 2020; 296:343-351.

38. Washino S, et al. Optimal PSA density thresholds for detecting csPCa in PI-RADS 3 lesions. Urology. 2018; 113:92-96.

39. Nordström T, et al. PSA thresholds for biopsy referral: population-based study. Eur Urol. 2015; 68:123-130.

40. National Comprehensive Cancer Network (NCCN). Clinical Practice Guidelines in Oncology: Prostate Cancer. Version 2024.

41. European Association of Urology (EAU). Guidelines on Prostate Cancer. 2024 Edition.

42. Loeb S, et al. Systematic review of complications after prostate biopsy. Eur Urol. 2013; 64:876-892.

43. Ehdaie B, et al. Incidence of sepsis following prostate biopsy in contemporary practice. J Urol. 2014; 192:702-709.

44. Castellani D, Pirola GM, Xi Y, et al. Infection rate after transperineal prostate biopsy with and without prophylactic antibiotics: results from a systematic review and meta-analysis of comparative studies. J Urol. 2021; 207.

45. Grummet J, Gorin MA, Popert R, et al. Transperineal versus transrectal prostate biopsy: a prospective multicenter randomized trial. Lancet Infect Dis. 2022; 22:1191-1199.

46. Xiang J, Yan H, Li J, et al. Comparison of transrectal and transperineal prostate biopsy approaches for infection risk: a systematic review and meta-analysis. J Urol. 2022; 207:220-229.

47. Bianchi L, Gandaglia G, Fossati N, et al. Infectious complications after transrectal prostate biopsy in the era of targeted prophylaxis. BJU Int. 2023; 131:214-223.

48. Cho S, Jun DY, Lee JY, et al. Comparison of urinary tract infection rates between transperineal prostate biopsies with and without prophylactic antibiotics: an updated systematic review and meta-analysis. Medicina (Kaunas). 2025; 61:198.

49. Ma F, Zhang Y. Antibiotic prophylaxis may still be required among transperineal prostate biopsies in diabetic patients: a cohort study. Front Med. 2025; 12:1618631.

Correspondence

Walid Shanaa
waleedshanea@yahoo.com

Omar Ali
oali@hamad.qa

Osama Abdeljaleel
OAbdeljaleel@hamad.qa

Ahmad Shamsodini
Aabbas@hamad.qa

Urology Section, Department of Surgery, Al Wakra Hospital,
Hamad Medical Corporation, Qatar

Ibrahim Alnadhari (Corresponding Author)
ibrahimah1978@yahoo.com

Urology Section, Department of Surgery, Al Wakra Hospital,
Hamad Medical Corporation, Qatar
Department of Surgery, Qatar University, Qatar

Hana J. Abukhadijah
HAbukhadijah@hamad.qa

Department of Surgery, Qatar University, Qatar